

UC Berkeley

UC Berkeley Previously Published Works

Title

Confusing Binaries: The Role of Stellar Binaries in Biasing Disk Properties in the Galactic Center

Permalink

<https://escholarship.org/uc/item/58v61996>

Journal

The Astrophysical Journal Letters, 853(2)

ISSN

2041-8205

Authors

Naoz, Smadar
Ghez, Andrea M
Hees, Aurelien
[et al.](#)

Publication Date

2018-02-01

DOI

10.3847/2041-8213/aaa6bf

Peer reviewed

CONFUSING BINARIES: THE ROLE OF STELLAR BINARIES IN BIASING DISK PROPERTIES IN THE GALACTIC CENTER

SMADAR NAOZ^{1,2}, ANDREA M. GHEZ¹, AURELIEN HEES¹, TUAN DO¹, GUNTHER WITZEL¹, JESSICA R. LU³

¹Department of Physics and Astronomy, University of California, Los Angeles, CA 90095, USA

²Mani L. Bhaumik Institute for Theoretical Physics, Department of Physics and Astronomy, UCLA, Los Angeles, CA 90095 and

³Astronomy Department, University of California, Berkeley, CA 94720, USA

Draft version January 15, 2018

ABSTRACT

The population of young stars near the Supermassive black hole (SMBH) in the Galactic Center (GC) has presented an unexpected challenge to theories of star formation. Kinematics measurements of these stars have revealed a stellar disk structure (with an apparent 20% disk membership) that has provided important clues to the origin of these mysterious young stars. However many of the apparent disk properties are difficult to explain, including the low disk membership fraction and the high eccentricities, given the youth of this population. Thus far, all efforts to derive the properties of this disk have made the simplifying assumption that stars at the GC are single stars. Nevertheless, stellar binaries are prevalent in our Galaxy, and recent investigations suggested that they may also be abundant in the Galactic Center. Here we show that binaries in the disk can largely alter the apparent orbital properties of the disk. The motion of binary members around each other adds a velocity component, which can be comparable to the magnitude of the velocity around the SMBH in the GC. Thus, neglecting the contribution of binaries can significantly vary the inferred stars' orbital properties. While the disk orientation is unaffected the apparent disk's 2D width will be increased to about 11.2° , similar to the observed width. For a population of stars orbiting the SMBH with zero eccentricity, unaccounted for binaries will create a wide apparent eccentricity distribution with an average of 0.23. This is consistent with the observed average eccentricity of the stars' in the disk. We suggest that this high eccentricity value, which poses a theoretical challenge, may be an artifact of binary stars. Finally, our results suggest that the actual disk membership might be significantly higher than the one inferred by observations that ignore the contribution of binaries, alleviating another theoretical challenge.

Keywords: stars: binaries: close, stars: black holes, kinematics and dynamics

1. INTRODUCTION

Recent observations in the Galactic Center (GC) revealed a population of young stars, which is consistent with a star formation episode $\sim 4-6$ Myr ago (the young nuclear cluster, YNC, e.g., Lu et al. 2009; Bartko et al. 2010; Do et al. 2013b,a; Feldmeier-Krause et al. 2015). These young stars appear to have two distinct kinematic structures around the Supermassive Black Hole (SMBH). Closer to the SMBH ($\lesssim 0.04$ pc) the stars have an isotropic distribution with high eccentricities (following a thermal distribution Gillessen et al. 2017) and may be slightly older as the highest mass stars are B stars (Ghez et al. 2003). These stars are the so called S-star cluster (e.g., Schödel et al. 2003; Ghez et al. 2005; Eisenhauer et al. 2005a; Ghez et al. 2008; Gillessen et al. 2009; Bartko et al. 2010; Yelda et al. 2014). Between ~ 0.04 pc and 0.5 pc, roughly 3/4 of the stars are old, late-type giants and the remaining 1/4 are young stars, including many massive Wolf-Rayet stars (Levin & Beloborodov 2003; Genzel et al. 2003; Eisenhauer et al. 2005b; Paumard et al. 2006; Lu et al. 2009; Bartko et al. 2009; Yelda et al. 2014).

Over time, the kinematic picture is becoming more precise as it has become possible to measure accelerations on the plane of the sky. Recently, Yelda et al. (2014), using high precision kinematic measurements and mod-

eling of 116 young stars in the inner ~ 1 pc of the GC, suggested that the stellar disk is composed of $\sim 20\%$ of the stars sampled between ~ 0.04 pc and 0.5 pc. The off-disk stellar population is less constrained and seems to be extended beyond ~ 0.1 pc ($\sim 3.2''$). The existence of additional substructure in this regime has been suggested (for example a warped disk), but it seems to have low significance (Bartko et al. 2009). Dynamical modeling of the stars in the disk yields an average stellar eccentricity of ~ 0.3 (Yelda et al. 2014). Moreover, the stars in the disk seem to follow a moderately top-heavy mass function (Bartko et al. 2010; Lu et al. 2013). In addition, the B stars in the disk have on average, similar kinematic properties as the more massive O and WR stars, suggesting a common star formation event (Lu et al. 2013).

The presence of the disk and its properties provide an important constraint to the origin of the young stars, which are hard to form in the inhospitable environment around the SMBH (e.g., Levin 2007). For example, it was suggested that the young S-star cluster might have formed further out in the disk and migrated in (e.g., Levin & Beloborodov 2003; Nayakshin 2006; Levin 2007; Alexander et al. 2008). Note, that there are many other ideas in the literature of the origin of the young stars in the GC, varying from breaking up binaries (e.g., Hills 1988; Yu & Tremaine 2003; Perets 2009), to collisions and mergers (e.g., Ginsburg & Loeb 2007; Antonini & Perets 2012; Stephan et al. 2016), and others (e.g., Perets et al.

2007; Hobbs & Nayakshin 2009; Perets et al. 2009). However, the kinematic substructure of the YNC, mentioned above, suggests that the cluster, and thus the young stars, formed in-situ rather than far from the SMBH (e.g., Berukoff & Hansen 2006; Lu et al. 2009; Yelda et al. 2014; Støstad et al. 2015; Feldmeier-Krause et al. 2015).

The stellar membership estimations and the modeling of the disk’s properties are based on multiple years of astrometric measurements, but typically only use *one* radial velocity (V_z) measurement (e.g., Bartko et al. 2009; Yelda et al. 2014). However, if at least some of the stars in the disk are in a binary configuration, the associate z-component velocity may be misleading, resulting in poor disk membership interpretation, and with larger apparent eccentricity around the SMBH than the physical one. Interestingly, among the stars with detected accelerations on the plane of the sky, which generally have the most robust disk membership estimate, the photometrically identified binary (Martins et al. 2006) IRS 16SW has the lowest disk membership probability (Yelda et al. 2014).

Recent observations have suggested that binaries are prevalent in our Galaxy ($\gtrsim 70\%$ for ABO spectral type stars, e.g., Raghavan et al. 2010). Thus, on face value, the binary fraction should be large among the young stars in the GC as well. So far, there have been three confirmed binaries in the inner ~ 0.2 pc of the GC. The first confirmed binary (IRS 16SW) is an equal-mass binary ($50 M_\odot$) at a projected distance estimated as ~ 0.05 pc with a period of 19.5 days (Ott et al. 1999; Martins et al. 2006; Rafelski et al. 2007). Recently, Pfuhl et al. (2013) discovered two additional binaries, an eclipsing Wolf-Rayet binary with a period of 2.3 days, and a long-period binary with an eccentricity of 0.3 and a period of 224 days. Both of these binaries are estimated to be at only ~ 0.1 pc from the SMBH. These observational studies suggest that the total massive binary fraction in the Young nuclear star cluster is comparable to the galactic one (e.g., Ott et al. 1999; Rafelski et al. 2007). Recently Stephan et al. (2016) showed that the binary fraction in the nuclear star cluster might be as high as 70%, compared to the initial binary fraction, following a star formation episode that took place in that region a few million years ago (e.g., Lu et al. 2013). Furthermore, other studies focusing on the overabundance of observed X-ray sources in the central 1pc suggests that compact binaries, involving stellar-mass BHs and neutron stars, may reside there in larger than average numbers (Muno et al. 2005). Together, these studies suggest that binaries are likely to be prevalent at the GC.

Several groups have begun to explore the dynamical effects of binaries (both stellar and compact objects) in shaping the physical properties of stellar distribution in the GC. For example, binaries are invoked to explain some long-standing observational puzzles, such as hypervelocity stars, the young stars in the S-cluster, the dark cusp, etc., (e.g., Hills 1988; Yu & Tremaine 2003; Antonini et al. 2010; O’Leary et al. 2009; Perets et al. 2009; Alexander & Hopman 2009; Antonini & Perets 2012; Alexander & Pfuhl 2013; Phifer et al. 2013; Prodan et al. 2015; Witzel et al. 2014, 2017; Stephan et al. 2016). Furthermore, it has been suggested that compact object binaries in the GC are a potential source of

gravitational wave emission (e.g., O’Leary et al. 2009; Antonini & Perets 2012; Prodan et al. 2015; Hoang et al. 2017).

Within the vicinity of a SMBH, the members of a stable binary have a tighter orbital configuration than the orbit of their mutual center of mass around the SMBH. In such a system, gravitational perturbations from the SMBH can induce large eccentricities on the binary orbit, which can cause the binary members to merge (see for review of the dynamics Naoz 2016). This coalescence may form a new star that can look like the G2 and G1 objects (Phifer et al. 2013; Prodan et al. 2015; Witzel et al. 2014, 2017; Stephan et al. 2016), which may eventually become blue stragglers (e.g., Naoz & Fabrycky 2014).

Here we suggest that some of the puzzling observations associated with the stellar disk may arise from neglecting the contribution of binaries to the kinematic measurements. Ignoring the contribution of binaries is known to cause an overestimation of the dynamical mass of star clusters (e.g. Kouwenhoven & de Grijs 2008). We demonstrate the importance of including binaries in the GC kinematic modeling by adopting a thin stellar disk with a population of binaries. We focus on the effects in inferring the disk’s properties as a result of neglecting the presence of these binaries. In particular, we show that ignoring the motion of binaries may lead to reduced disk membership and an increased apparent eccentricity and semi-major axis of the stars in the disk. We present our initial conditions in Section 2 and present the spirant biases and disk properties in Section 3, and finally, discuss our results and implication in Section 4.

2. INITIAL CONDITIONS FOR DISK BINARIES

We present a proof-of-concept calculation of the effect of the binary motion on the apparent orbital parameters. We assume a razor thin stellar disk around a $4 \times 10^6 M_\odot$ SMBH (e.g., Ghez et al. 2008; Boehle et al. 2016; Gillessen et al. 2017). We model the disk extending from 0.04 pc to 0.5 pc around the SMBH. The semi-major axis of the orbit around the SMBH (a_2) is chosen to have a Bahcall-Wolf-like distribution with the number density $n(r) \sim r^{-2}$ (as supported by observations, e.g., Lu et al. 2009; Støstad et al. 2015). Note that the number of stars in a shell can be written as $dN = 4\pi r^2 n(r) dr$, and thus the choice of the semi-major axis around the SMBH follows a uniform distribution in a_2 (i.e., constant dN/dr) between 0.04 pc and 0.5 pc. We adopt Yelda et al. (2014) orbital parameters for the disk location on the Sky. Specifically, we set $i_D = 130^\circ$ and $\Omega_D = 96^\circ$. The angle i_D is the inclination with respect to the observer, such that $\cos i_D = h_z/h_D$, where h_z is the z-component of the angular momentum of a star \mathbf{h}_D and h_D is the magnitude of the stellar orbital angular momentum around the SMBH. The z axis is along the line of sight and the observer is located at $z = -8.32$ kpc (e.g., Gillessen et al. 2017). In the first simulation, each binary star system is assigned to be on a circular velocity around the SMBH (i.e., $e_D = 0$ for all the orbits). In a second simulations, the binaries are put on orbits around the SMBH with $e_D = 0.3$. The nominal, default, case we consider throughout the paper is the case for $e_D = 0$, and we will refer to the eccentric case for comparison in our results. We model a total of 80,000 systems for two disk’s eccentricity choices (40,000 per choice of disk’s ec-

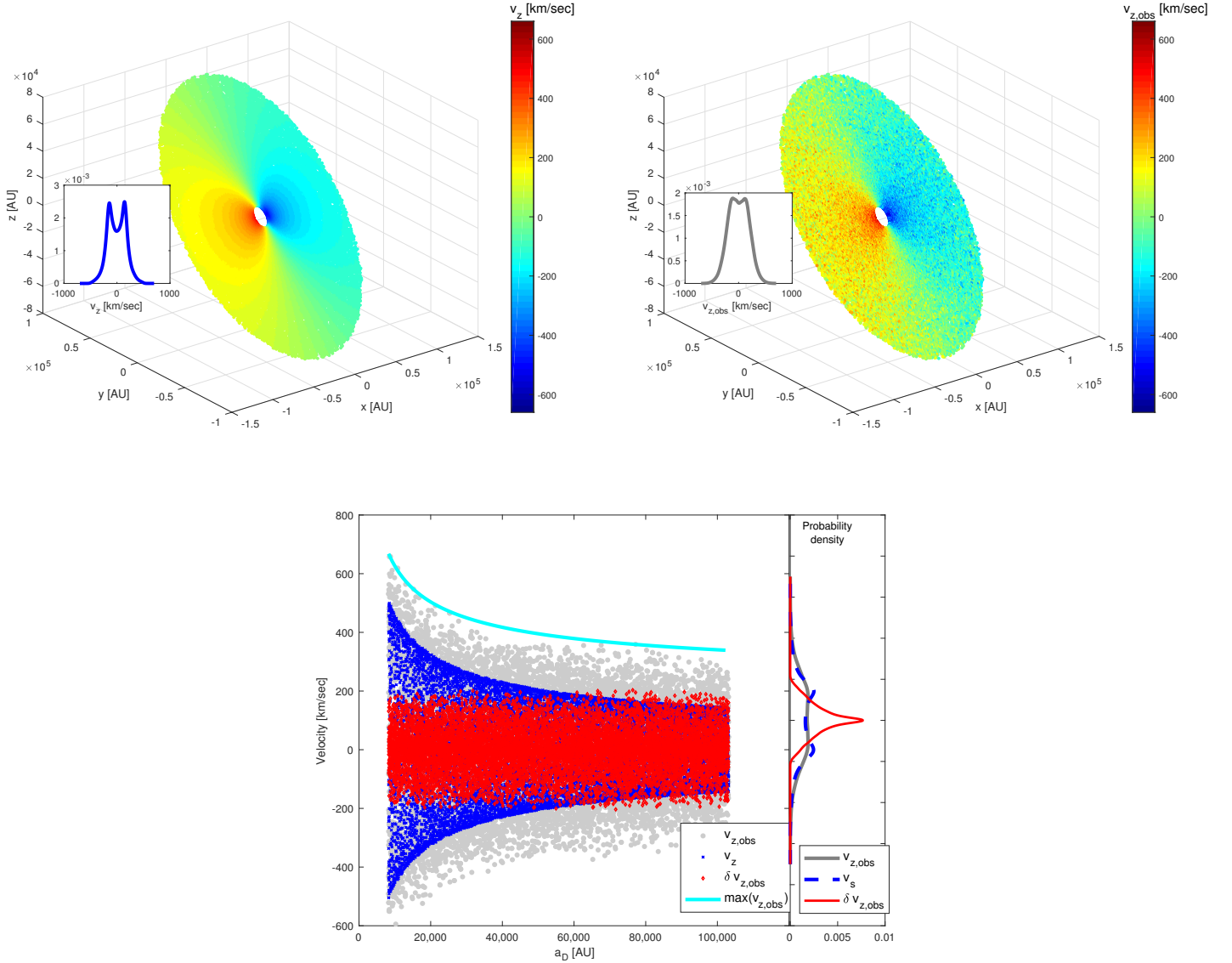


Figure 1. *Top panels:* 3D representation of the disk. *Top left panel:* stars in the disk, without accounting for the binaries’ affect on the velocity. The inset shows the distribution of the the v_z component for the binaries’ center of mass motion around the SMBH. *Top right panel:* stars in the disk while accounting for binaries affect on the velocities. The color code shows the observed z -component velocities for binary stars, i.e., $v_{z,obs} = v_z + \delta v_{z,obs}$. The inset shows the distribution of the z -component velocity of these binary stars around the SMBH. *Bottom panel* shows the z -component velocity as a function of the stellar disk’s semi-major axis a_D . We show the input velocity v_z (blue), the induced wobble $\delta v_{z,obs}$ (red) and the observed part $v_{z,obs} = v_z + \delta v_{z,obs}$. For illustrative purposes we show only 20% from the Monte-Carlo simulations. The cyan line shows the maximum value of $v_{z,obs}$. We show the associated probability densities of these quantities in the right bottom panel. Note that unless said explicitly, we consider the $e_D = 0$ case.

centricity) and for each system use a uniform distribution to chose (1) the argument of periapsis of the orbit around the SMBH, ω (0° to 360°) and (2) the mean anomaly of the orbit around the SMBH (0° to 180°), from which we find the true anomaly for the circular and eccentric cases. Given these orbital parameter we can find the location ($\mathbf{r}_D = (x, y, z)$) and velocity ($\mathbf{v}_D = (v_x, v_y, v_z)$) of the stars in the disk (e.g., Murray & Dermott 2000). We note that compared to the Murray & Dermott (2000) transformation, the observation convention is such that $x \rightarrow y$ and $y \rightarrow -x$. This convention corresponds to having the origin of the longtime of ascending nodes (Ω) in

the north, corresponding to positive x (e.g., Ghez et al. 2005). The top left panel in Figure 1 shows the 3D representation of the disk, color coded by the z -component of the velocities around the SMBH, v_z .

We assume that every star in the disk is actually a $m = 10 M_\odot$ star with a binary companion, with a mass ratio q . The mass ratio was chosen from a uniform distribution between 0 and 1 to match the distributions of the Galactic O star population (e.g., Sana & Evans 2011; Sana et al. 2012). We assume that all the binaries are on a circular orbit with a semi-major axis of 0.1 AU (e.g., Li et al. 2017; Chu et al. 2017, Ginsburg et al in prep.),

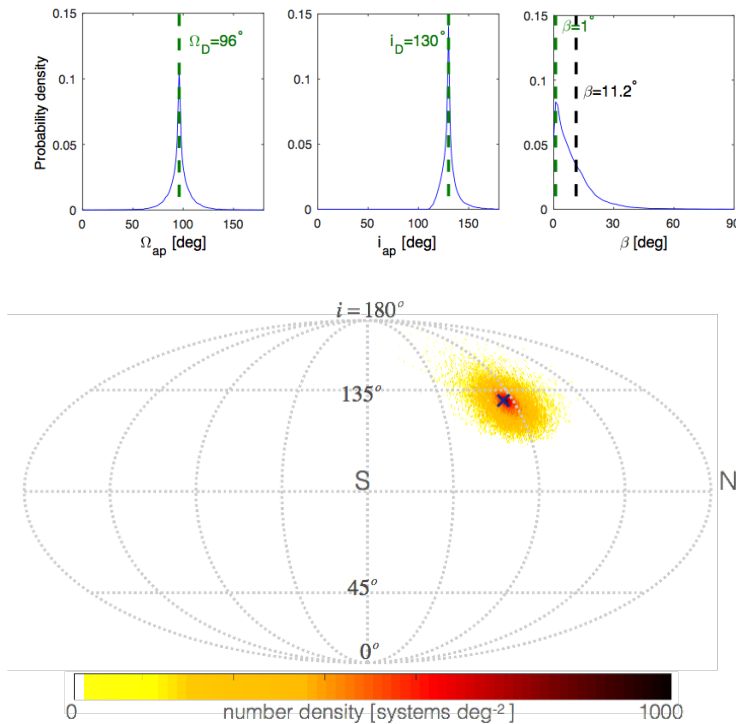


Figure 2. *Top row:* The density probability of the apparent orbital parameters as a result of the binary wobble. We show the (right from left) the apparent ascending nodes (Ω_{ap}), inclination, (i_{ap}), and the quantity β . No change in the parameters yields a zero tilt angle. The green dashed lines in each panel mark the peak of the distribution. The black dashed line represents the β angle associated with 68% of the population (see text). *Bottom panel:* Apparent sky projection of the disk in an equal area Mollweide projection. The direction of the normal vector is described by the inclination (i_{ap}), depicts here by horizontal lines spaced 45° apart and the angle to the ascending node (Ω_{ap}) longitudinal lines spaced 45° apart, with the line marked N representing 0° . The razor thin initial disk was set to be at $(i_D, \Omega_D) = (130^\circ, 96^\circ)$. The color shows the density of systems in 0.2 square degree pixel area. The light blue X marks the maximum density peak disk value, which corresponds to i_D and Ω_D . We also note that some systems do exist in the left half sphere of the sky-projection plot, but the density is very low corresponding to light yellow in the color palette.

which sets the binary period to be $P = 3.6/\sqrt{1+q}$ days. Larger separations are more sensitive to eccentricity excitations due to the Eccentric Kozai-Lidov (EKL) mechanism as they yield shorter EKL timescale compared to General Relativity¹, which can lead to merging the two binary members (e.g., Stephan et al. 2016; Li et al. 2017). Furthermore, gravitational perturbations from fly-by stars that eventually can unbind the binary (e.g., Binney & Tremaine 1987). Thus, we adopt a hard binary (e.g., Quinlan 1996) with 0.1 AU separation as a proof-of-concept. The induced observed wobble of the primary at the z-direction², due to the binary, (either positive or negative) is then (for a binary on a circular

¹ Note that comparable precession timescale between General Relativity and EKL can still cause eccentricity excitations in the form of resonant behavior, (e.g., Naoz et al. 2013) thus we have chosen a much larger difference in the timescales.

² Note that velocity wobble due to the stellar companion may also be observable because of the flat mass ratio distribution. For simplicity, we ignore this contribution, and assume that these companions are fainter than the primaries.

orbit around it’s center of mass)

$$\delta v_{z,\text{obs}}^3 = 2\pi G \frac{q^3}{(1+q)^2} \frac{m}{P} \sin^3 i_{\text{bin}} \cos^3 f_{\text{bin}}, \quad (1)$$

where i_{bin} is the binary inclination, drawn from a isotropic distribution between $0 - 180^\circ$ (i.e., uniform in $\cos i_{\text{bin}}$), f_{bin} is the true anomaly of the binary, and G is the gravitational constant. Each orbit on the disk with a velocity vector \mathbf{v}_D will have an additional observed velocity component along the z direction $\delta \mathbf{v}_z$. In other words the observed velocity will be $\mathbf{v}_{\text{obs}} = \mathbf{v}_D + \delta \mathbf{v}_{z,\text{obs}}$.

Note that our choose of a random binary mass ratio, binary phase and inclination, reduces the impact of the binaries. On the other hand we fixed the binary separation and assumed a circular binary. Allowing for a distribution of binary separations might increase in some cases and decrease in others the wobble value. Thus, we do not expect a qualitatively change the results of this proof-of-concept calculations.

The wobble velocity $\delta \mathbf{v}_{z,\text{obs}}$ will be at the order of \mathbf{v}_D at characteristic distances from the SMBH

$$a_{D,c} \sim a_1 \frac{M}{m} \frac{1+q}{q^2} \frac{1}{\sin i_{\text{bin}}} \sim 8 \times 10^4 \left(\frac{M}{4 \times 10^6 M_\odot} \right) \text{ AU} \quad (2)$$

For example a typical value for a star in the disk is $\sim 200 \text{ km sec}^{-1}$ (see inset in the left panel of Figure 1), and a typical wobble for these massive binaries are $\sim 100 \text{ km sec}^{-1}$ see Figure 1. Therefore, the resulted observed z-component velocity spread on somewhat larger range and has different velocity distribution (see Figure 1, top right panel). Binaries that are closer to the SMBH will be less sensitive to the additional velocity induced by the binary. As depicted in Figure 1, further away from the SMBH the Keplerian velocity around the SMBH may be comparable to that of the binary wobble and thus can greatly affect the inferred orbital properties.

3. DISK PROPERTY BIASES INDUCED BY BINARIES

Given this “new” observed velocity component we can find the “observed” (apparent) orbital parameters. In other words, treating a binary system as a single star can result in inferring orbital parameters that are inconsistent with the physical ones. Specifically, we are interested in Ω_{ap} and i_{ap} , where the subscript “ap” stand for apparent. We calculate the apparent angular momentum \mathbf{h}_{ap} and thus, the angles can be easily found using the following relations (e.g., Murray & Dermott 2000):

$$\cos i_{\text{ap}} = \frac{h_{z,\text{ap}}}{h_{\text{ap}}}, \quad (3)$$

and

$$\cos \Omega_{\text{ap}} = \frac{-h_{y,\text{ap}}}{h_{\text{ap}} \sin i_{\text{ap}}} \quad \text{and} \quad \sin \Omega_{\text{ap}} = \frac{h_{x,\text{ap}}}{h_{\text{ap}} \sin i_{\text{ap}}}. \quad (4)$$

We show the probability density of these angles in Figure 2 top panels³. As expected the resulted angles have a wide distribution that peaks at the disk value, i.e., $i_D = 130^\circ$ and $\Omega_D = 96^\circ$. These values are close to the median

³ The probability density is calculated based on a normal kernel function, and is evaluated at equally-spaced points of the relevant angle.

of the distributions. However, due to the long tail the averages are different. Specifically, we find, $\langle i_{\text{ap}} \rangle \sim 130.6^\circ$ and $\langle \Omega_{\text{ap}} \rangle \sim 95.6^\circ$ with standard deviations of $\sim 7.8^\circ$ and $\sim 15^\circ$ respectively. These angles define the location of the disk on a sky, and in Figure 2, bottom panel, we show the apparent sky projection, color coded with the density of stars from our simulations. We define the density as the number of stars in a degree area of $i_{\text{ap}} \times \Omega_{\text{ap}}$. Note that the maximum density takes place at i_D and Ω_D , marked by light blue X in the bottom Figure of 2, as indicated in the probability distribution in the top of Figure 2. Note the slight “shadow” near the X is a result of over-density of slightly dark pixels and it corresponds to roughly 1σ of disk membership (see below). The spread around the razor thin disk is the result of the relative motion of the binaries around each other. Interestingly, the density of the apparent disk members around the maximum, projected on the sky, is not dissimilar from the observations (see for example Yelda et al. 2014, figure 10).

We define a quantity

$$\beta = \sqrt{(\Omega_{\text{ap}} - \Omega_D)^2 + (i_{\text{ap}} - i_D)^2}, \quad (5)$$

which can be used as a proxy for disk membership (see below). In Figure 2, top right panel we show probability density of β which peaks at 1° . The deviation from a peak at $\beta = 0^\circ$ can be understood from the asymmetry of the inclination distribution. In terms of the number systems, the peak of this distribution for i_{ap} is about a factor of two smaller than that for Ω_{ap} . Combining i_{ap} and Ω_{ap} yields β . We found that the average $\langle \beta \rangle \sim 10.1^\circ$ with a standard deviation of 13.5° . Because the peak distributions in Ω_{ap} and i_{ap} are similar to the initial disk input, the apparent peak density of stars in the sky projected disk (bottom panel in Figure 2) is at the initial disk input (marked by the light blue X). Below we adopt the disk membership by estimating the critical angle β_{68} at which 68% of the systems lay within it around the disk, which corresponds to $\beta_{68} = 11.2^\circ$. The 68% from the initial disk’s input (i.e., $\beta = 0$) is shown in the vertical dashed black line in Figure 2.

We also calculate the apparent eccentricity in the disk using Kepler relation, i.e.,

$$e_{\text{ap}} = \sqrt{1 - \frac{h_{\text{ap}}^2}{G(M + m(1 + q))a_{\text{ap}}}}, \quad (6)$$

where M is the SMBH mass and a_{ap} is found from the following Kepler relation

$$\frac{1}{a_{\text{ap}}} = \frac{2}{r_D} - \frac{v_{\text{obs}}^2}{G(M + m(1 + q))}. \quad (7)$$

We show the distribution of the apparent semi-major axis and eccentricity in Figure 3, top left and right panels, respectively. As depicted in this Figure, closer to the SMBH, the apparent semi-major axis roughly follows the razor thin input disk distribution (the latter depicted in black dashed line). At radii larger than ~ 0.2 pc the apparent semi-major axis distribution significantly deviates from the initial input, where the a_{ap} is inferred to have much larger values than the input ones. As can be seen from Equation (7) large observed velocity yields

a larger apparent semi-major axis of the stars around the SMBH than they actually are (left panel in Figure 3).

Note that the projected distance of the disk (i.e., $\sqrt{x^2 + y^2}$) is independent on the binary velocity component. In particular, as depicted in Figure 3, disk membership drops to $\sim 50\%$ for radii larger than the projected $6.5''$. The latter projected distance is often used in observation to determine the disk location. The results from our proof-of-concept calculations are consistent with the observed high disk membership inside $\sim 3.2''$ (e.g., Yelda et al. 2014). In particular, we consider the 116 stars with kinematic data from Yelda et al. (2014), who estimated that about 20% of the stars reside on the disk. We find the likelihood value, presented in Yelda et al. (2014), that is associated with setting the sum over all fraction of stars in the disk, in each bin, to 20%, as shown in the bottom panel of Figure 3, black line⁴. As depicted, the observations show the same sky projected trend as our simulations, where stars closer to the SMBH have larger *assigned* disk membership. This similarity in trend suggests that the binary fraction in the galactic center is rather large. In fact, taking this analysis at face value, the results presented here suggest that the disk fraction should be higher by a factor of 2.5 (estimated roughly from the comparison between the red and black lines in Figure 3). Thus, suggesting a possible *true* disk fraction of $\sim 50\%$ ⁵. It is interesting to point out that the confirmed binary IRS 16SW, which has a detected acceleration and which resides rather close to the inner edge of the SMBH (the first bin from the left, in the plot) is the only star at the inner disk edge with a low disk membership probability.

The stars in the razor thin disk were set with $e_D = 0$, but their apparent eccentricity distribution has a wide range with an average of ~ 0.23 and standard deviation of 0.2, taking only bound orbits. The probability distribution is depicted in Figure 3, right panel, solid blue line. Furthermore, we also found that about 3% of the inferred systems resulted in eccentricities that are nearly radial or completely unbound on hyperbolic orbit. This may explain the observed high eccentricity and the nearly radial orbits reported by Bartko et al. (2009). Taking only the disk members in our simulation (i.e., either $\beta \leq 11.2^\circ$), we plot their eccentricity’s probability distribution in Figure 3, top right panel. The average disk members’ eccentricity is 0.14 with standard deviation of 0.13. Thus, our simulations suggest that perhaps some of the observed eccentric stars may actually have a circular orbit around the SMBH, and their eccentricity is only inferred to be high, as a result from the induced z-component velocity of a binary.

We also take Yelda et al. (2014) reported eccentricity at face value and repeat the above exercise for initial $e_D = 0.3$. We found that all the above angles (i.e., i_{ap} , Ω_{ap} , α and β) produce similar probability distribution,

⁴ We emphasize that we did not use Yelda et al. (2014) uncertainties estimations, instead we reduced their likelihood to assigned disk membership which allows to a “cleaner” comparison with our calculations.

⁵ The fraction of disk membership is estimated by summing over all of the bins, i.e., $\sum n\Delta a_2/\Delta a_{\text{Disk}}$, where n is the number of stars in the disk inside of projected bin Δa_2 (in linear scale). We then divide by the total linear projected length of the disk ($\Delta a_{\text{Disk}} \sim 0.46$ pc).

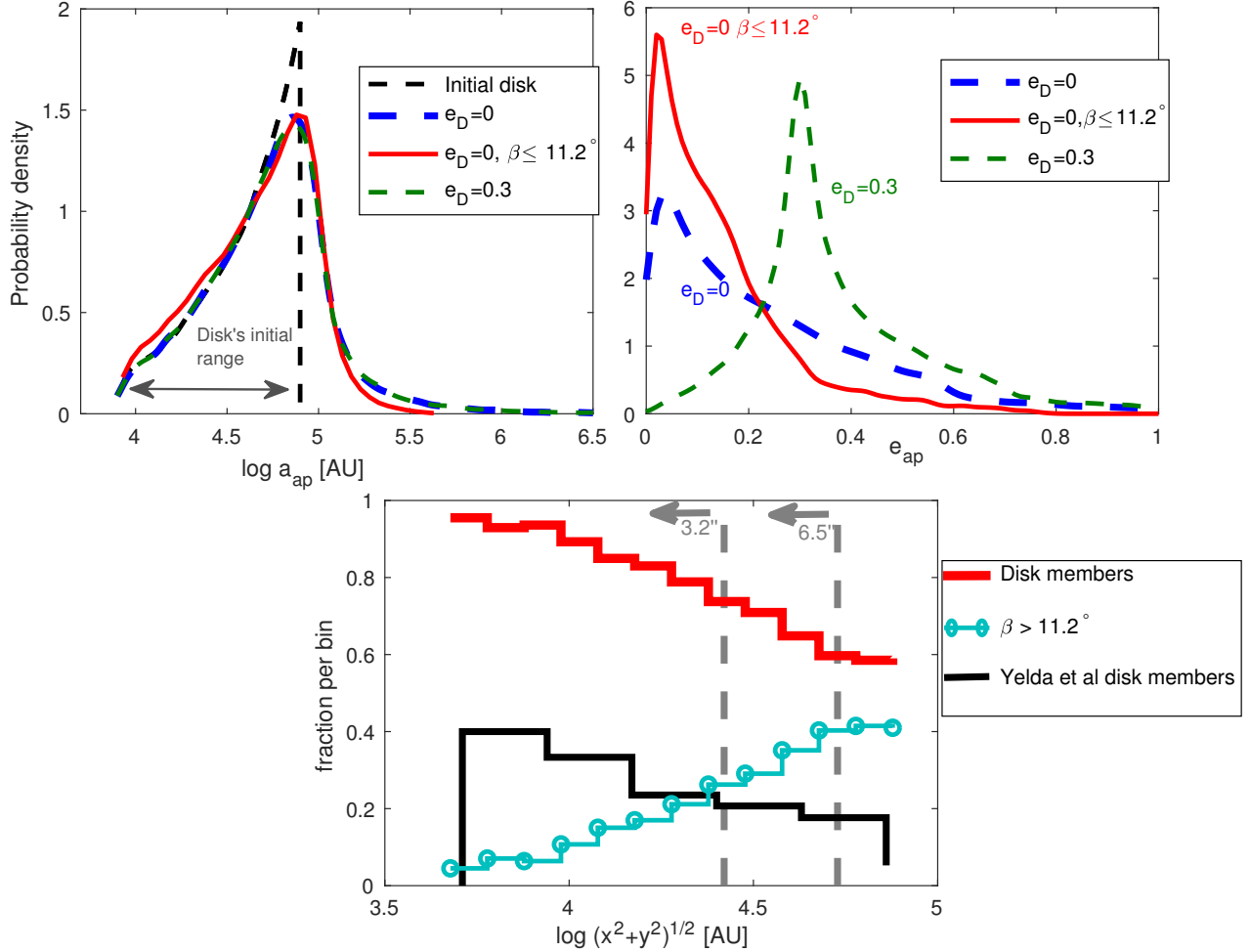


Figure 3. *Top row:* The density probability of the apparent semi-major axis (a_{ap}), left panel, and the apparent eccentricity (e_{ap}), right panel. We show the two cases associated with two different initial eccentricities for each star in the disk, $e_D = 0$ (blue dashed lines) and $e_D = 0.3$ (green dashed lines). The two initial eccentricity cases give the same density probabilities for the angles in Figure 2. The dashed gray line in the left panel shows the probability density of the initial disk and its range. The solid red lines show the disk members' eccentricity (right) and a_{ap} (left) density probability for the $e_D = 0$ run. Disk members are defined as those with $\beta \leq 11.2^\circ$ (i.e., β_{68}). *Bottom panel:* The fraction of stars in the disk (red line) represented as stars with $\beta \leq 11.2^\circ$ (solid line). Stars with $\beta > 11.2^\circ$ are inferred to lay outside the disk (solid, cyan line). The black line shows the disk members estimated from the 116 stars from Yelda et al. (2014). The observed disk membership is normalized such that 20% of the stars reside in the disk (see text). Overplotted are the sky projected radius bins at $3.2''$ and $6.5''$ when assuming a distance to the SMBH of 8.32 kpc. Note that the observed disk membership per projected distance bin and our calculations show the same trend, with a ~ 2.5 difference. This similarity implies that the disk membership might be as high as $\sim 50\%$ instead of the inferred $\sim 20\%$ fraction achieved while ignoring binaries.

and thus are omitted from the Figures to avoid clutter. On the other hand the inferred eccentricity probability distribution is different (as depicted in Figure 3, green dashed lines), with an average of 0.4 and a standard deviation of 0.24, taking only bound orbits. About 3% of systems resulted on a hyperbolic orbits in this case. As illustrate in this Figure, if the orbits around the SMBH were indeed eccentric, the binary contribution would have implied an apparent eccentricity, with an even higher values. This may explain the large eccentricities reported in the literature (e.g., Bartko et al. 2009; Yelda et al. 2014).

While Ω , i and β are sky projected quantities, we are also interested in the physical tilt between the input disk's angular momentum and the resulted apparent disk. Thus, we calculate the relative deflection angle α between the actual stellar disk's angular momentum \mathbf{h}_D

and the apparent one \mathbf{h}_{ap} where

$$\cos \alpha = \frac{\mathbf{h}_D \cdot \mathbf{h}_{\text{ap}}}{h_D h_{\text{ap}}}, \quad (8)$$

The distribution of this angle is shown in the inset of Figure 4. This distribution peaks around $\sim 1^\circ$ with an average of 8° with a standard deviation of 8° . In other words, a razor thin disk appears to be puffed when the mutual motion of the binaries is neglected. In addition to that, the disk appears tilted compared to its actual orientation as the peak of α is not oriented at zero.

The stars' Keplerian orbits imply that binaries that are further away from the disk, have smaller velocity around the SMBH compared to stars that are closer to the SMBH (see Figure 1). Thus, the stars that are closer to the SMBH will have smaller deflection angle (i.e., $\cos \alpha \sim 1$) relative to the stars that are further away

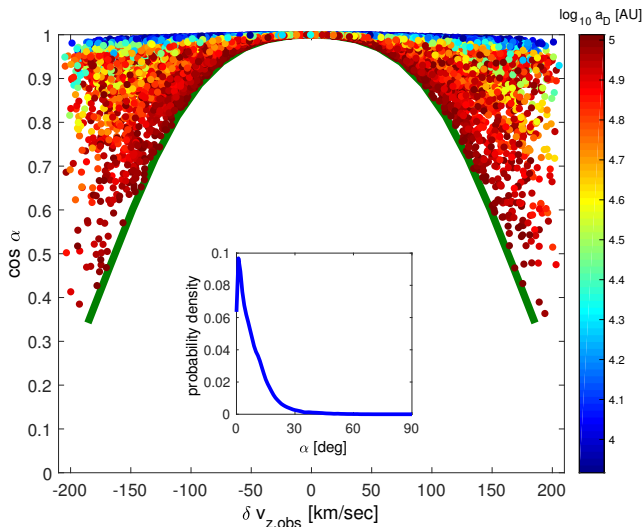


Figure 4. The angle between the two angular momenta (α) as a function of the binary radial velocity. The different color corresponds to the input semi-major axis of each binary around the SMBH in log space. The green solid line shows the analytical Equation (9). The inset show α distribution.

in the disk. We depict this behavior in Figure 4, where the larger deflection angles are associated with larger semi-major axes (a_D) from the SMBH. From vectorial identities, and using the fact that the binary velocity excess is observed only in the z -component (i.e., $\Delta = \delta v_{z,\text{obs}}/v_D$), we can write:

$$\cos \alpha = \frac{1 + (v_z/v_D)\Delta}{\sqrt{1 + 2(v_z/v_D)\Delta + (x^2 + y^2)/r_D^2 \Delta^2}}, \quad (9)$$

and in terms of the inclination and longitude of ascending nodes we can write:

$$\cos \alpha = \sin i_D \sin i_{\text{ap}} \cos(\Omega_D - \Omega_{\text{ap}}) + \cos i_D \cos i_{\text{ap}}. \quad (10)$$

In Figure 4, we show the analytical relation from Equation (9) for the far edge of the disk 0.5 pc, and the maximum v_z/v_D in the disk (which is about 0.77). Large α can be mistakenly interpreted as if stars lay outside the plane of the disk. As expected, the error in estimating the stellar disk's membership (small β and thus small α , from Eq. (10)) is highly correlated with the distance from the SMBH. Stars that have wider orbit around the SMBH need larger $\delta v_{z,\text{obs}}$ to produce larger variations in α , and thus are less likely to be sensitive to binary configuration.

4. DISCUSSION AND CONCLUSIONS

We have shown that the binarity nature of stars can significantly influence the apparent (observed) stellar disk properties in the GC. The stellar disk in the GC is estimated to be located between 0.04 pc and 0.5 pc, with sky projected inclination of $i_D = 130^\circ$ ascending nodes of $\Omega_D = 96^\circ$ (Yelda et al. 2014). Since the determination of disk membership is often estimated by one RV measurement, a velocity wobble on the z -axis (the line-of-sight) due to the binary motion can change the apparent properties.

We have conducted a simple proof-of-concept calculation that considered a razor-thin disk around the SMBH

in the GC, assuming that each star is, in a binary configuration (see Figure 1). The apparent physical and projected orbital parameter are substantially different compared to the input one. For example, the inclination and ascending nodes deduced when ignoring the possibilities of an extra z -component that arises from the binary motion results in a wide distribution for these angles (as depicted in Figure 2). The width of the distribution is largely caused by the velocity distribution, which is sensitive to the binary mass ratio and binary orientation (both drawn from a uniform distributions). The binary motion causes the apparent location of the disk to be slightly shifted from the input location (as shown in Figure 2 bottom panel). Note that we assumed a 100% binary fraction in the disk, as we have fixed all values which are model dependent (e.g., binary fraction and binaries eccentricity and separation distribution). These effects may change the quantitative results presented here (e.g., a distribution of binary separations may increase the effect) but not the qualitative effect.

As expected disk members that are farther away from the SMBH will be more sensitive to the binary motion than those that are closer to the SMBH since the latter have larger orbital velocity v_D . The binary wobble velocity along the line of sight cause a system to appear off the disk and further away from the SMBH than truly is. In particular, we are more likely to deduce that stars that are closer to the SMBH belong to the disk, than those that are initially further away from the SMBH. This behavior is shown in Figure 3, bottom panel, and remarkably, this trend is consistent with observations, depicts as the black line in this Figure. Considering the observations, we find that the binary IRS 16SW, which resides rather close to the SMBH, was found to have low probability to reside in the disk (Yelda et al. 2014), consistent with our finding.

We note that Yelda et al. (2014) showed that observational sampling and prior assumptions can have large impact on the probability of disk membership. Using a forward modeling approach, they find that observations along the line of nodes of the disk along with uniform acceleration priors in the analysis can result in an over prediction for the disk by a factor of 2. Future quantitative comparisons with this work will likely need to account for similar types of observational biases.

Furthermore, the disk eccentricity may appear different than the actual orbital eccentricity. Starting with circular orbits around the SMBH, we found that the apparent eccentricity around the SMBH significantly differs from zero (see Figure 3, right panel). Interestingly, the apparent disk's eccentricity distribution (blue line in Figure 3) has a mean value of ~ 0.26 , which is consistent with Yelda et al. (2014) estimation from observations. The apparent disk eccentricity can reach extreme values and even results in an apparent unbound orbits, which is also consistent with observations (e.g., Bartko et al. 2009). Not only the disk's eccentricity will deviate from the physical one, but also the disk's members semi-major axis. Ignoring the contribution from binary motion will cause many disk members to appear more distant from the SMBH than they actually are (see Figure 3 left panel).

We defined a disk membership condition using a quantity that roughly describes an angular distance from the

disk location on the sky, β , in the longitude of ascending nodes, Ω and the inclination, i , plane. We estimate the disk membership by considering the systems that lay within β_{68} (i.e., corresponding to 68% of systems around the initial location of the disk). As expected, we find that the disk fraction decreases as a function of the projected distance (e.g., Figure 3, bottom panel). This trend is consistent with the observations, as shown in that Figure, black line. This functional agreement, suggests that binaries are more prevalent in the Galactic Center and may result in reducing the disk membership. Taking on face value our initial conditions and comparing our results to observations, may suggest that disk membership can be as high as $\sim 50\%$.

We conclude that the possibility of existing binaries in the measurements of the stellar disk properties cannot be ignored. As we showed, many of the puzzles and controversies involved the characteristics of the disk may be explained by the existence of binaries. We encourage the community to take more measurements of the z-component of the stars' velocities.

We thank the referee for his/her useful comments. S.N and A.M.G thank the Keck foundation for their partial support of the *NStarsOrbits* Project. S.N. acknowledges partial support from a Sloan Foundation Fellowship. A.M.G thanks the NSF grant number AST-1412615.

REFERENCES

- Alexander, R. D., Armitage, P. J., Cuadra, J., & Begelman, M. C. 2008, *ApJ*, 674, 927
- Alexander, T. & Hopman, C. 2009, *ApJ*, 697, 1861
- Alexander, T. & Pfuhl, O. 2013, *ArXiv e-prints*
- Antonini, F., Faber, J., Gualandris, A., & Merritt, D. 2010, *ApJ*, 713, 90
- Antonini, F. & Perets, H. B. 2012, *ApJ*, 757, 27
- Bartko, H., Martins, F., Fritz, T. K., Genzel, R., Levin, Y., Perets, H. B., Paumard, T., Nayakshin, S., Gerhard, O., Alexander, T., Dodds-Eden, K., Eisenhauer, F., Gillessen, S., Mascetti, L., Ott, T., Perrin, G., Pfuhl, O., Reid, M. J., Rouan, D., Sternberg, A., & Trippe, S. 2009, *ApJ*, 697, 1741
- Bartko, H., Martins, F., Trippe, S., Fritz, T. K., Genzel, R., Ott, T., Eisenhauer, F., Gillessen, S., Paumard, T., Alexander, T., Dodds-Eden, K., Gerhard, O., Levin, Y., Mascetti, L., Nayakshin, S., Perets, H. B., Perrin, G., Pfuhl, O., Reid, M. J., Rouan, D., Zilka, M., & Sternberg, A. 2010, *ApJ*, 708, 834
- Berukoff, S. J. & Hansen, B. M. S. 2006, *ApJ*, 650, 901
- Binney, J., & Tremaine, S. 1987, Princeton, NJ, Princeton University Press, 1987, 747 p.,
- Boehle, A., Ghez, A. M., Schödel, R., Meyer, L., Yelda, S., Albers, S., Martinez, G. D., Becklin, E. E., Do, T., Lu, J. R., Matthews, K., Morris, M. R., Sitarski, B., & Witzel, G. 2016, *ApJ*, 830, 17
- Chu, D. S., Do, T., Hees, A., Ghez, A., Naoz, S., Witzel, G., Sakai, S., Chappell, S., Gautam, A. K., Lu, J. R., & Matthews, K. 2017, *ArXiv e-prints*
- Do, T., Lu, J. R., Ghez, A. M., Morris, M. R., Yelda, S., Martinez, G. D., Wright, S. A., & Matthews, K. 2013a, *ApJ*, 764, 154
- Do, T., Martinez, G. D., Yelda, S., Ghez, A., Bullock, J., Kaplinghat, M., Lu, J. R., Peter, A. H. G., & Phifer, K. 2013b, *ApJ*, 779, L6
- Eisenhauer, F., Genzel, R., Alexander, T., Abuter, R., Paumard, T., Ott, T., Gilbert, A., Gillessen, S., Horrobin, M., Trippe, S., Bonnet, H., Dumas, C., Hubin, N., Kaufer, A., Kissler-Patig, M., Monnet, G., Ströbele, S., Szeifert, T., Eckart, A., Schödel, R., & Zucker, S. 2005a, *ApJ*, 628, 246
- . 2005b, *ApJ*, 628, 246
- Feldmeier-Krause, A., Neumayer, N., Schödel, R., Seth, A., Hilker, M., de Zeeuw, P. T., Kuntschner, H., Walcher, C. J., Lützgendorf, N., & Kissler-Patig, M. 2015, *A&A*, 584, A2
- Genzel, R., Schödel, R., Ott, T., Eisenhauer, F., Hofmann, R., Lehnert, M., Eckart, A., Alexander, T., Sternberg, A., Lenzen, R., Clénet, Y., Lacombe, F., Rouan, D., Renzini, A., & Tacconi-Garman, L. E. 2003, *ApJ*, 594, 812
- Ghez, A. M., Duchêne, G., Matthews, K., Hornstein, S. D., Tanner, A., Larkin, J., Morris, M., Becklin, E. E., Salim, S., Kremenek, T., Thompson, D., Soifer, B. T., Neugebauer, G., & McLean, I. 2003, *ApJ*, 586, L127
- Ghez, A. M., Salim, S., Hornstein, S. D., Tanner, A., Lu, J. R., Morris, M., Becklin, E. E., & Duchêne, G. 2005, *ApJ*, 620, 744
- Ghez, A. M., Salim, S., Weinberg, N. N., Lu, J. R., Do, T., Dunn, J. K., Matthews, K., Morris, M. R., Yelda, S., Becklin, E. E., Kremenek, T., Milosavljevic, M., & Naiman, J. 2008, *ApJ*, 689, 1044
- Gillessen, S., Eisenhauer, F., Trippe, S., Alexander, T., Genzel, R., Martins, F., & Ott, T. 2009, *ApJ*, 692, 1075
- Gillessen, S., Plewa, P. M., Eisenhauer, F., Sari, R., Waisberg, I., Habibi, M., Pfuhl, O., George, E., Dexter, J., von Fellenberg, S., Ott, T., & Genzel, R. 2017, *ApJ*, 837, 30
- Ginsburg, I. & Loeb, A. 2007, *MNRAS*, 376, 492
- Hills, J. G. 1988, *Nature*, 331, 687
- Hoang, B.-M., Naoz, S., Kocsis, B., Rasio, F. A., & Dosopoulou, F. 2017, *ArXiv e-prints*
- Hobbs, A. & Nayakshin, S. 2009, *MNRAS*, 394, 191
- Kouwenhoven, M. B. N., & de Grijs, R. 2008, *A&A*, 480, 103
- Levin, Y. 2007, *MNRAS*, 374, 515
- Levin, Y. & Beloborodov, A. M. 2003, *ApJ*, 590, L33
- Li, G., Ginsburg, I., Naoz, S., & Loeb, A. 2017, *ApJ*, 851, 131
- Lu, J. R., Do, T., Ghez, A. M., Morris, M. R., Yelda, S., & Matthews, K. 2013, *ApJ*, 764, 155
- Lu, J. R., Ghez, A. M., Hornstein, S. D., Morris, M. R., Becklin, E. E., & Matthews, K. 2009, *ApJ*, 690, 1463
- Martins, F., Trippe, S., Paumard, T., Ott, T., Genzel, R., Rauw, G., Eisenhauer, F., Gillessen, S., Maness, H., & Abuter, R. 2006, *ApJ*, 649, L103
- Muno, M. P., Lu, J. R., Baganoff, F. K., Brandt, W. N., Garmire, G. P., Ghez, A. M., Hornstein, S. D., & Morris, M. R. 2005, *ApJ*, 633, 228
- Murray, C. D. & Dermott, S. F. 2000, *Solar System Dynamics*, ed. Murray, C. D. & Dermott, S. F.
- Naoz, S. 2016, *ARA&A*, 54, 441
- Naoz, S. & Fabrycky, D. C. 2014, *ApJ*, 793, 137
- Naoz, S., Kocsis, B., Loeb, A., & Yunes, N. 2013, *ApJ*, 773, 187
- Nayakshin, S. 2006, *MNRAS*, 372, 143
- O'Leary, R. M., Kocsis, B., & Loeb, A. 2009, *MNRAS*, 395, 2127
- Ott, T., Eckart, A., & Genzel, R. 1999, *ApJ*, 523, 248
- Paumard, T., Genzel, R., Martins, F., Nayakshin, S., Beloborodov, A. M., Levin, Y., Trippe, S., Eisenhauer, F., Ott, T., Gillessen, S., Abuter, R., Cuadra, J., Alexander, T., & Sternberg, A. 2006, *ApJ*, 643, 1011
- Perets, H. B. 2009, *ApJ*, 698, 1330
- Perets, H. B., Gualandris, A., Kupi, G., Merritt, D., & Alexander, T. 2009, *ApJ*, 702, 884
- Perets, H. B., Hopman, C., & Alexander, T. 2007, *ApJ*, 656, 709
- Pfuhl, O., Alexander, T., Gillessen, S., Martins, F., Genzel, R., Eisenhauer, F., Fritz, T. K., & Ott, T. 2013, *ArXiv e-prints*
- Phifer, K., Do, T., Meyer, L., Ghez, A. M., Witzel, G., Yelda, S., Boehle, A., Lu, J. R., Morris, M. R., Becklin, E. E., & Matthews, K. 2013, *ApJ*, 773, L13
- Prodan, S., Antonini, F., & Perets, H. B. 2015, *ApJ*, 799, 118
- Quinlan, G. D. 1996, *NA*, 1, 35
- Rafelski, M., Ghez, A. M., Hornstein, S. D., Lu, J. R., & Morris, M. 2007, *ApJ*, 659, 1241
- Raghavan, D., McAlister, H. A., Henry, T. J., Latham, D. W., Marcy, G. W., Mason, B. D., Gies, D. R., White, R. J., & ten Brummelaar, T. A. 2010, *ApJS*, 190, 1
- Sana, H., & Evans, C. J. 2011, *Active OB Stars: Structure, Evolution, Mass Loss, and Critical Limits*, 272, 474
- Sana, H., de Mink, S. E., de Koter, A., et al. 2012, *Science*, 337, 444
- Schödel, R., Genzel, R., Ott, T., & Eckart, A. 2003, *Astronomische Nachrichten Supplement*, 324, 535
- Stephan, A. P., Naoz, S., Ghez, A. M., Witzel, G., Sitarski, B. N., Do, T., & Kocsis, B. 2016, *MNRAS*, 460, 3494
- Støstad, M., Do, T., Murray, N., Lu, J. R., Yelda, S., & Ghez, A. 2015, *ApJ*, 808, 106

Witzel, G., Ghez, A. M., Morris, M. R., Sitarski, B. N., Boehle, A., Naoz, S., Campbell, R., Becklin, E. E., Canalizo, G., Chappell, S., Do, T., Lu, J. R., Matthews, K., Meyer, L., Stockton, A., Wizinowich, P., & Yelda, S. 2014, ApJ, 796, L8

Witzel, G., Sitarski, B. N., Ghez, A. M., Morris, M. R., Hees, A., Do, T., Lu, J. R., Naoz, S., Boehle, A., Martinez, G., Chappell, S., Schödel, R., Meyer, L., Yelda, S., Becklin, E. E., & Matthews, K. 2017, ArXiv e-prints
Yelda, S., Ghez, A. M., Lu, J. R., Do, T., Meyer, L., Morris, M. R., & Matthews, K. 2014, ApJ, 783, 131
Yu, Q. & Tremaine, S. 2003, ApJ, 599, 1129